

# Generating Symmetry in the Asymmetric ATP-binding Cassette (ABC) Transporter Pdr5 from *Saccharomyces cerevisiae*\*

Received for publication, January 27, 2014, and in revised form, March 24, 2014. Published, JBC Papers in Press, April 14, 2014, DOI 10.1074/jbc.M114.553065

Rakeshkumar P. Gupta, Petra Kueppers, Nils Hanekop, and Lutz Schmitt<sup>1</sup>

From the Institute of Biochemistry, Heinrich Heine University Düsseldorf, Universitätsstrasse 1, 40225 Düsseldorf, Germany

**Background:** Fungal multidrug efflux pumps possess a degenerate nucleotide-binding site (NBS).

**Results:** Restoring all the nonconserved amino acids in the degenerate NBS of Pdr5 leads to complete loss of function of the protein.

**Conclusion:** The degenerate NBS is essential and acts as a structural platform supporting the canonical NBS.

**Significance:** This is the first study dealing with the entire degenerate NBS and its functional role.

Pdr5 is a plasma membrane-bound ABC transporter from *Saccharomyces cerevisiae* and is involved in the phenomenon of resistance against xenobiotics, which are clinically relevant in bacteria, fungi, and humans. Many fungal ABC transporters such as Pdr5 display an inherent asymmetry in their nucleotide-binding sites (NBS) unlike most of their human counterparts. This degeneracy of the NBSs is very intriguing and needs explanation in terms of structural and functional relevance. In this study, we mutated nonconsensus amino acid residues in the NBSs to its consensus counterpart and studied its effect on the function of the protein and effect on yeast cells. The completely “regenerated” Pdr5 protein was severely impaired in its function of ATP hydrolysis and of rhodamine 6G transport. Moreover, we observe alternative compensatory mechanisms to counteract drug toxicity in some of the mutants. In essence, we describe here the first attempts to restore complete symmetry in an asymmetric ABC transporter and to study its effects, which might be relevant to the entire class of asymmetric ABC transporters.

ABC<sup>2</sup> transporters are found in all kingdoms of life; in prokaryotes they function as importers (1) and exporters, although they mainly act as exporters in eukaryotes (2, 3). Multidrug resistance (MDR) during chemotherapy in the treatment of cancer or in immunocompromised individuals has made the biochemical and structural study of these proteins essential. In fungi, many ABC transporters have been at the center of scientific investigation, for example, their involvement in the phenomenon of pleiotropic drug resistance (4), a phenomena similar to MDR.

Pdr5 is an ABC transporter localized in the plasma membrane of bakers' yeast, *Saccharomyces cerevisiae*. It is a functional homologue of P-gp (MDR1 or ABCB1), which is the most widely studied ABC transporter from humans (5). Pdr5 is involved in the extrusion of a wide variety of xenotoxic compounds from the cell (6–8). It is a full-size transporter having two nucleotide-binding domains (NBDs) and two transmembrane domains (TMDs) displaying an NBD-TMD-NBD-TMD membrane topology. This is inverse to that of the classic topology of ABC transporters (TMD-NBD-TMD-NBD). Since the discovery that a mutation in the transcription factor, which controls the expression of this membrane protein, leads to overexpression of Pdr5 (9), it has turned out to be an important model for studying MDR or to be more precise pleiotropic drug resistance as it is called in yeast.

Pdr5 displays a high basal ATPase activity, which, unlike its other human counterparts such as P-gp, does not seem to be stimulated in the presence of substrates (7, 10). Such an uncoupling has important mechanistic consequences because ATP hydrolysis is supposed to be the crucial step that triggers the transport of substrates across the membrane, and in the proper environment, it is strictly coupled to substrate translocation (11). The NBDs play the role of harnessing chemical energy from ATP and converting it to mechanical energy by inducing structural changes in the TMDs to extrude the substrate to the exterior of the cell (12, 13). The amino acid residues involved in binding and hydrolysis of ATP are essential for the proper functionality of the protein. A number of previous studies have investigated the roles of individual and groups of amino acids in the NBDs and shed light on their roles during ATP binding and hydrolysis. As per the generally accepted model, an ABC transporter binds two nucleotides in the two NBDs. This binding occurs in a head-to-tail fashion, *i.e.* consensus residues from Walker A (GXGXXGKST, where X can be any amino acid) and Walker B ( $\phi\phi\phi\phi$ DE, where  $\phi$  can be any hydrophobic amino acid) motifs as well as the H-loop (XHX) from one NBD and the C-loop (LSGGQ) from the other NBD sandwich one ATP molecule between them, thereby forming the nucleotide-binding site (NBS) (12). Once both nucleotides are bound at the two NBSs, the transporter is supposed to switch from the so-called

\* This work was supported by Deutsche Forschungsgemeinschaft Grant Schm1279/5-3 and European Drug Initiative on Channels and Transporters FP7 Theme Health-2007–2.1.1.-5 (to L. S.).

<sup>1</sup> To whom correspondence should be addressed. Tel.: 49-211-81-10773; Fax: 49-211-81-15310; E-mail: lutz.schmitt@hhu.de.

<sup>2</sup> The abbreviations used are: ABC, ATP-binding cassette; NBS, nucleotide-binding site; NBD, nucleotide-binding domain; OM, oligomycin; MDR, multidrug resistance; TMD, transmembrane domain; R6G, rhodamine 6G; P-gp, p-glycoprotein.

TABLE 1

List of primers used for introducing point mutations in *pdr5* gene on pRE5 plasmid

S is sense, and AS is antisense.

Mutation	Direction	Sequence, 5' to 3'
P195S	S	GCTAGTCGTTTTAGGTAGATCAGGCTCTGGCAAAAC
	AS	GTTTTGCCAGAGCCTGATCTACCTAAAACGACTAGC
C199K	S	CGTTTTAGGTAGACCAGGCTCTGGCAAACTACTTTATTTAAATCCATCTCTTC
	AS	GAAGAGATGGATTTTAAATAAAGTAGTTTGGCCAGAGC CTGGTCTACCTAAAACG
N334E	S	GATCCAAATTTCAATGCTGGGATGAAGCTACAAGG GTTTGGATTCT
	AS	GAATCCAACCCCTTGTAGCTTCATCCAGCATTGAA ATTTGGATC
Y367H	S	CTGCCACAGTGGCCATCCATCAATGTCTCAAGATG
	AS	CATCTTGAGAACATTGATGGATGGCCACTGTGGCAG
N1011S	S	GTTGTGGTGTGCTGGTGAAGGTTTATCTGTTGAAC AAAGAAAAAGATTAACCATTG
	AS	CAATGGTTAATCTTTTTCTTTGTTCAACAGATAAACCT TCACCAGCAACACCAACAAC
V1012G	S	GTTGCTGGTGAAGGTTTAAACGGTGAACAAGAAAA AGATTAACC
	AS	GGTTAATCTTTTTCTTTGTTCCACCGTTTAAACCTTCAC CAGCAAC
E1013G	S	GTTGCTGGTGAAGGTTTAAACGGTGGTCAAAGAAAA GATTAACCATTGGTG
	AS	CACCAATGGTTAATCTTTTTCTTTGACCAACGTTTAAA CCTTCACCAGCAAC

inward-facing to the so-called outward-facing conformation, and as a consequence of this conformational change, the substrate is extruded (14). Moreover, ATP hydrolysis has been suggested to be the step that sets the transporter back to the inward-facing conformation ready to accept new substrate molecules for the next cycle of substrate translocation (14). However, there is debate about the number of ATP molecules that are hydrolyzed for one cycle of transport to be completed. But the prerequisite for both bound ATP molecules to be hydrolyzed is the presence of key consensus residues in both NBSs. As seen in Fig. 1, Pdr5 lacks key residues in one of the two NBSs. Although this degenerate site could bind ATP, hydrolysis should be impossible or severely impaired due to the absence of these key residues. Some initial mutational studies supported this view (10). This observation of a degenerate and a consensus site is common in yeast ABC transporters but is uncommon in ABC transporters of archaea and bacteria. In the case of human counterparts, only TAP1/2 (ABC B2/B3) and many transporters of the subfamily C display this sort of degeneration (15). A well studied example of a eukaryotic protein possessing a degenerate NBS is the cystic fibrosis transmembrane regulator. Here, site 1 (degenerate) is proposed to be bound to ATP through many cycles of ATP hydrolysis occurring at site 2 (canonical) and thus play a supporting role (16). This leads us to question the functional relevance for the protein and on a broader scale to the cell for maintaining a degenerate NBS, because such evolutionary conservation of this trait in yeast ABC transporters does need an explanation. In this study, we systematically interchanged each degenerated amino acid residue in the NBSs and studied its effect on the functionality of the protein and in turn on the cellular consequences.

## EXPERIMENTAL PROCEDURES

**Liquid Drug Assay**—Ketoconazole, fluconazole, and rhodamine 6g (R6G) were obtained from Sigma, and cycloheximide was obtained from Fluka. All drug stock solutions were prepared in dimethyl sulfoxide (DMSO, Acros Organics), and further dilutions were carried out in sterile water. Assay was carried out in sterile 96-well microtiter plates (Falcon) with 20  $\mu$ l of drug, 180  $\mu$ l of YPD medium, and 50  $\mu$ l of  $A_{620}$  0.2 yeast culture. Plates were incubated at 30 °C for 48 h, and  $A_{620}$  was measured with an ELISA plate reader (FLUOstar-Optima). No further correction was applied as none of the used drugs displayed an absorption to 620 nm.

**Yeast Strains and Plasmid Mutagenesis**—Yeast strains were cultured in YPD medium containing 10 g/liter yeast extract, 20 g/liter peptone, and 2% glucose. The following *S. cerevisiae* strains were used in this study: YALF-A1 (*MATa: ura3-52 trp 1-1 leu 2-3, his 3-11, 15 ade 2-1 PDR 1-3*), YHW-A5 (*MATa: ura3-52 trp 1-1 leu 2-3, his 3-11, 15 ade 2-1 PDR 1-3 pdr5 $\Delta$ ::TRP1*), and YRE1001 (*MATa: ura3-52 trp 1-1 leu 2-3, his 3-11, 15 ade 2-1 PDR 1-3 pdr5pdr5prom $\Delta$ ::TRP1*). Details about plasmid and strain construction can be found in Table 1 and Ref. 10. Site-directed mutagenesis of *pdr5* was performed on plasmid pRE5 with the QuikChange II XL site-directed mutagenesis kit (Stratagene).

**Isolation of Plasma Membranes**—Cells were grown in YPD medium at 30 °C. At  $A_{620}$  of 1.5, the nitrogen source was replenished by addition of a 10th volume of 5 $\times$  YP (50 g/liter yeast extract; 100 g/liter tryptone/peptone). Cells were harvested at  $A_{600}$  of 3.5. The isolation of plasma membranes was performed as described elsewhere (8, 10).

**Rhodamine 6G Transport Assay**—Active R6G transport was recorded according to the protocol developed by Kolaczowski and co-workers (17), using a FluoroLog III fluorescence spectrometer (Horiba). Isolated plasma membranes (30  $\mu$ g of total protein content) were resuspended in 1 ml of transport buffer (50 mM Hepes (pH 7.0), 10 mM MgCl<sub>2</sub>, 150 nM R6G, and 10 mM azide) and incubated at 35 °C. Transport was initiated by addition of 10 mM ATP. In the presence of ATP, Pdr5 transports R6G from the outside to the inside of the membrane vesicle due to its inside-out orientation (NBDs face outside). R6G accumulation into the vesicle leads to self-quenching and results in the overall decrease in fluorescence intensity. The final relative decrease in fluorescence intensity is representative of the relative  $V_{max}$  for transport of the dye.

**ATPase Activity Assays**—Oligomycin (OM)-sensitive ATPase activity of plasma membrane fractions was measured by a colorimetric assay performed in 96-well microtiter plates (9, 17, 18). Isolated plasma membranes (0.1 or 0.2  $\mu$ g per well) were incubated with 4 mM ATP, 5 mM MgCl<sub>2</sub> in 300 mM Tris-glycine buffer (pH 9.0) in a final volume of 25  $\mu$ l. To reduce background, 0.2 mM ammonium molybdate, 50 mM KNO<sub>3</sub>, and 10 mM Na<sub>2</sub>N<sub>3</sub>, respectively, were added (9, 19). In a control reaction, OM (20  $\mu$ g/ml) was added to the assay to determine the OM-sensitive ATPase activity. After incubation at 30 °C for 20 min, the reaction was stopped by addition of 175  $\mu$ l of ice-cold

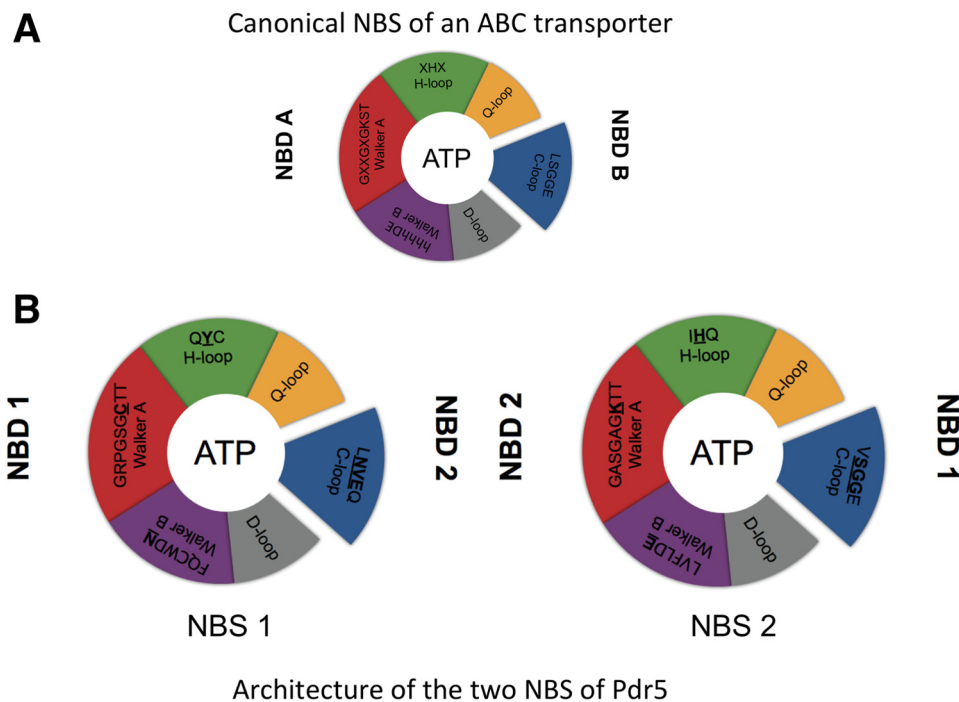


FIGURE 1. **Schematic architecture of NBS.** A, canonical NBS of ABC transporters. B, NBS1 and NBS2 of *Pdr5*.

40 mM H<sub>2</sub>SO<sub>4</sub>. The amount of released inorganic phosphate was determined by a colorimetric assay, using Na<sub>2</sub>HPO<sub>4</sub> as standard (20).

## RESULTS

A classic or canonical NBS of an ABC transporter is composed of residues of the Walker A and Walker B motifs, the Q-loop, D-loop, and H-loop from one NBD and the C-loop of the opposing NBD forming a so-called composite ATP-binding site (Fig. 1A). Based on structural studies of P-loop NTPases (21), the lysine of the Walker A motif coordinates the  $\beta$ - and  $\gamma$ -phosphate moiety of ATP, and the aspartate residue of the Walker B motif interacts with the cofactor Mg<sup>2+</sup> (12, 22, 23), which is essential for hydrolytic activity. The glutamate residue of the Walker B motif and the histidine residue of the H-loop are essential for ATPase activity and are shown to form a catalytic dyad (24, 25). However, in the case of *Pdr5*, mutation of the histidine in NBS2 did not reduce or even abolish ATPase activity as shown for many other ABC systems (see Zaitseva *et al.* (12, 25 and reference therein)), rather it selectively influenced the spectrum of transported substrates (10). The serine and second glycine residue of the C-loop of the opposing NBD interact with the  $\gamma$ -phosphate moiety of ATP and complete the NBS. Furthermore, the glutamine residue of the Q-loop also coordinates directly or indirectly the cofactor Mg<sup>2+</sup>. Although the D-loop is thought to be involved in NBD-NBD communication in the composite dimer. Here, we excluded the D-loop and the Q-loop from our experiments. An elegant study already investigated the role of the Q-loop in NBD-TMD cross-talk of *Pdr5*, where it was seen that the mutation of Q-loop residues from the deviant and consensus part of NBDs led to drug hypersensitivity and displayed functional redundancy, while maintaining significant ATPase activity (26). Hence, we focused only

on the important residues of the Walker A and B motifs, the H-loop, and the C-loop for this study.

**Mutagenesis in *Pdr5***—Mutations to replace degenerate amino acid residues with their consensus counterparts were done in a stepwise fashion. The complete list of mutations is summarized in Table 2. Site-directed mutagenesis was performed in pRE5 plasmid after which the *pdr5* gene was subsequently excised and transformed into the *Saccharomyces* strain  $\Delta pdr5\Delta pdr5prom$ , where by homologous recombination the *pdr5* gene is chromosomally integrated (10). In this background, this leads to constitutive expression of *Pdr5* under the strong *pdr5* promoter. In the following, restoration of the consensus sequence in the Walker A motif (C199K) located in NBD1 and forming NBS1 is called the “Walker A” mutant; restoration of the consensus sequence in the Walker B motif (N334E; NBD1) in NBS1 is called the “Walker B” mutant; restoration of the consensus sequence of the H-loop (Y367H, NBD1) in NBS1 is called the “H-loop” mutant, and restoration of the consensus sequence of the C-loop (N1011S/V1012G/E1013G, NBD2) in NBS1 is called the “C-loop” mutant. The corresponding combinations are called “HC-loop” (H- and C-loop mutations), AHC (H- and C-loop as well as Walker A mutations), and ABHC (H- and C-loop as well as Walker A and Walker B mutations). Please note that in the context of the combined mutations affecting the Walker A motif of NBS1, we also exchanged the proline residue at position 195 to a serine residue. We speculated that proline within the Walker A motif might hamper its functionality in wrapping around the phosphate moiety of the bound nucleotide. However, on the level of the single mutation, no difference to the single C199K mutant was detected. Nevertheless, we kept this exchange in the combined mutations.

TABLE 2

List of mutations generated and used in this study

Mutation	Abbreviation	Alteration	Motif	Domain
P195S		Pro in Walker A	Walker A	NBD1
C199K	Walker A	Cys in Walker A	Walker A	NBD1
N334E	Walker B	Asn in Walker B	Walker B	NBD1
Y367H	H-loop	Tyr in H-loop	H-loop	NBD1
N1011S, V1012G, E1013G	C-loop	Asn, Val, and Glu in C-loop	C-loop	NBD2
Y367H, N1011S, V1012G, E1013G	HC-loop	Tyr in H-loop Asn, Val, and Glu in C-loop	H-loop C-loop	NBD1/2
C199K	AHC	Cys in Walker A	Walker A	NBD1/2
Y367H		Tyr in H-loop	H-loop	
N1011S, V1012G, E1013G		Asn, Val, and Glu in C-loop	C-loop	
P195S	ABHC	Pro in Walker A	Walker A	NBD1/2
C199K		Cys in Walker A	Walker B	
N334E		Asn in Walker B	H-loop	
Y367H		Tyr in H-loop	C-loop	
N1011S, V1012G, E1013G		Asn, Val, and Glu in C-loop		

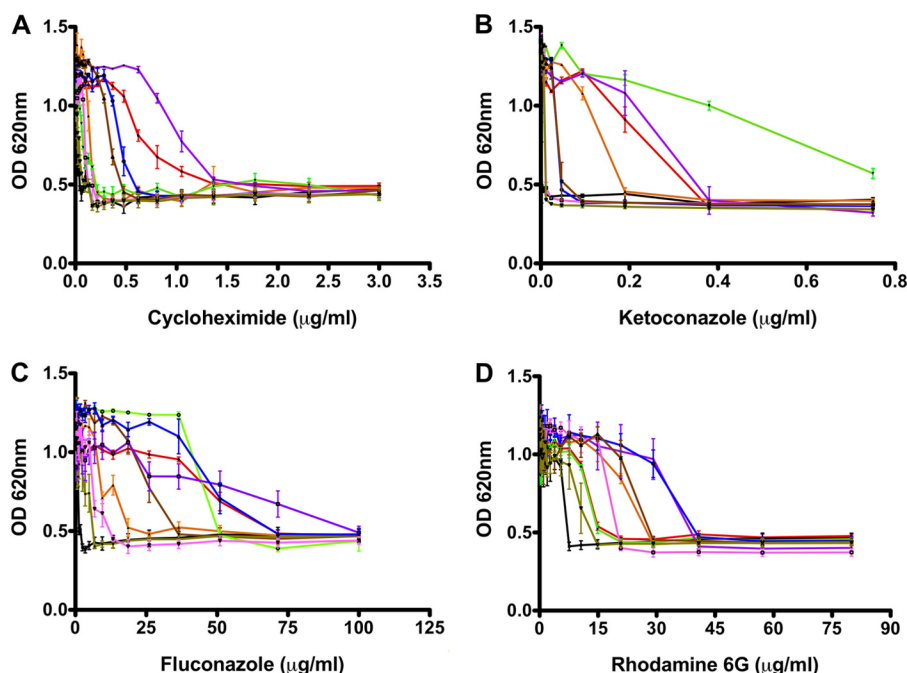


FIGURE 2. **Liquid drug resistance assay.** Cell growth of Pdr5 mutants was analyzed after 48 h of incubation at 30 °C with cycloheximide (A), ketoconazole (B), fluconazole (C), and R6G (D). Color coding is as follows: red, Pdr5WT; black,  $\Delta$ Pdr5; orange, Walker A; green, Walker B; purple, H-loop; blue, C-loop; brown, HC-loop; dark green, AHC-loop; and magenta, ABHC-loop.

**Liquid Drug Resistance Assay**—To determine the effects of mutations in key residues of the NBDs, we investigated the changes in resistance toward specific drugs belonging to different classes. As an internal control and reference for the absence of resistance, the  $\Delta$ pdr5 strain was employed. The response of the mutants toward these drugs was interestingly not uniform. For cycloheximide (Fig. 2A), the H-loop mutant displayed a stronger resistance as compared with wild type; for theazole drug, ketoconazole (Fig. 2B), Walker B and H-loop mutants were more resistant than wild type; for fluconazole (Fig. 2C), the Walker B, H-loop, and C-loop mutants displayed stronger resistance as compared with wild type. Finally, for R6G (Fig. 2D), the Walker A, H-loop, C-loop, HC-loop, and the ABHC mutants displayed higher resistance. Noticeably, the ABHC mutant, which contained all conserved residues and thereby restored a symmetrical architecture of the two NBDs, was severely impaired in providing better resistance toward all drugs except for R6G.

**In Vitro OM-sensitive ATPase Assay**—ATPase activity tests were carried out, to investigate the biochemical basis for such altered drug resistance of the mutants. For this purpose, Pdr5-enriched plasma membranes were isolated using the Serrano protocol (27). Fig. 3 demonstrated that the expression levels in the plasma membrane of all mutants were very similar if not identical to wild type levels. Therefore, the differences in resistance patterns observed in the liquid drug assay cannot be attributed to differences in the amounts of protein being expressed.

OM-sensitive ATPase activity was measured colorimetrically by determining the amount of inorganic phosphate released over time by the malachite green assay. The results are summarized in Fig. 4. As clearly seen, all mutants except the AHC and ABHC mutants displayed ATPase activity comparable with wild type with a 2-fold increase in apparent affinity at maximum for the H-loop mutant. Moreover, a quantitative analysis of the kinetic parameters of ATP hydrolysis revealed

## Role of Degenerate Nucleotide-binding Site in Pdr5

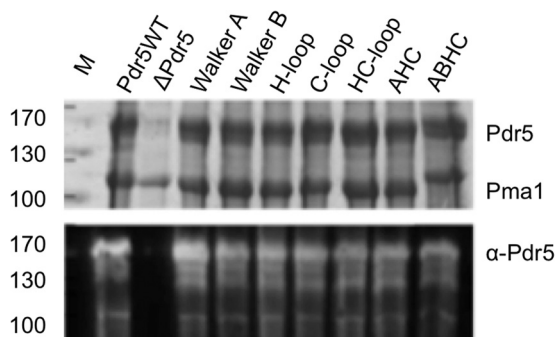


FIGURE 3. **Expression levels of Pdr5 mutants.** Upper panel, Coomassie Blue-stained SDS-PAGE of plasma membrane preparations of *S. cerevisiae* cells expressing wild type Pdr5 (*Pdr5WT*), no Pdr5 ( $\Delta$ ), or the different NBD mutations. 15  $\mu$ g of total protein amount were applied per lane. Molecular masses of marker proteins are indicated at left (*M*). Bands corresponding to Pdr5 and the plasma membrane ATPase Pma1 are indicated. Lower panel, detection of Pdr5 variants by Western blot analysis employing a polyclonal  $\alpha$ -Pdr5 antibody.

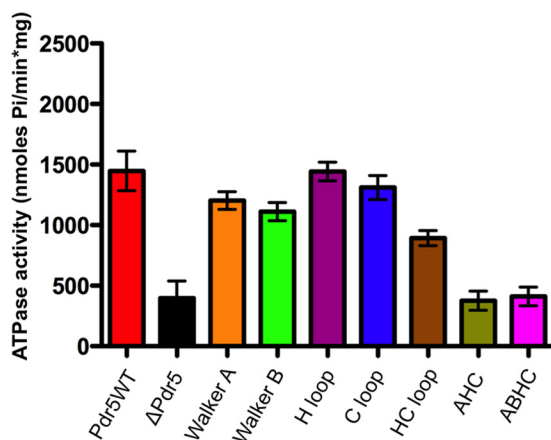


FIGURE 4. **OM-sensitive ATPase activity of Pdr5 mutants.** The assay was performed with 0.1 or 0.2  $\mu$ g of protein and incubation at 30  $^{\circ}$ C for 20 min. The released inorganic phosphate was detected by the malachite green assay for  $P_i$  determination. (See "Experimental Procedures" for assay details.)

**TABLE 3**  
Kinetics of ATPase activity of Pdr5 mutants

$K_m$  and  $V_{max}$  values derived from Michaelis-Menten analysis of the OM-sensitive ATPase data for wild type Pdr5 and the different mutants

Mutant	$K_m$	$V_{max}$
	<i>mM</i>	$\mu$ mol/min*mg
Pdr5 WT	1.71 $\pm$ 0.71	1.33 $\pm$ 0.23
Walker A	1.06 $\pm$ 0.27	1.50 $\pm$ 0.13
Walker B	1.97 $\pm$ 0.50	1.15 $\pm$ 0.13
H-loop	4.08 $\pm$ 1.49	2.09 $\pm$ 0.46
C-loop	1.36 $\pm$ 0.46	1.33 $\pm$ 0.17
HC-loop	1.04 $\pm$ 0.23	1.37 $\pm$ 0.10
AHC	1.19 $\pm$ 0.75	0.48 $\pm$ 0.97
ABHC	1.80 $\pm$ 0.50	0.20 $\pm$ 0.03

that the apparent affinity of these mutants toward ATP has not drastically changed (Table 3). Only the AHC and ABHC mutants were severely impaired in their maximal reaction velocity ( $V_{max}$ ) of ATP hydrolysis and displayed values comparable with the negative control ( $\Delta pdr5$ -containing strains).

**In Vitro R6G Transport Assay**—An *in vitro* R6G transport assay presents an elegant readout of the functional integrity of Pdr5 in inside-out membrane vesicles. The assay is based on the principle of transport of R6G molecules to the inner leaflet or the lumen of the vesicle in the presence of an energy source, *i.e.*

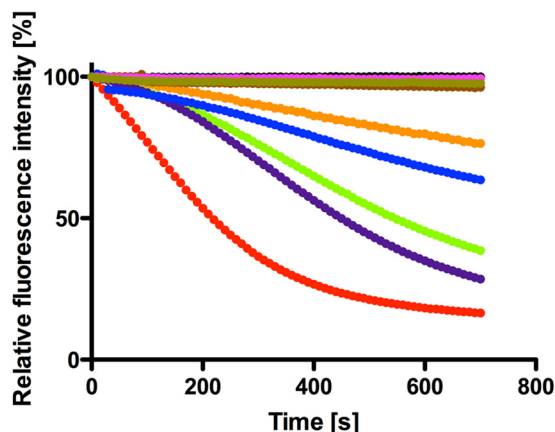


FIGURE 5. **In vitro R6G transport activity of Pdr5 mutants.** Reaction mixture contained 20  $\mu$ g of protein, 300 nM R6G, 10 mM  $MgCl_2$ , 10 mM  $NaN_3$ , and 10 mM ATP. Reaction was initiated by addition of ATP, which leads to Pdr5-mediated transport of the dye from outside to inside the membrane vesicle. This accumulation of dye leads to self-quenching and an overall decrease in fluorescence intensity, which is monitored using a spectrofluorometer (Horiba, FluoroLog III) and is indicative of Pdr5 activity. Color-coding of mutants is the same as in Fig. 2.

**TABLE 4**  
Kinetics of *in vitro* R6G transport activity of Pdr5 mutants

$K_m$  values calculated from Michaelis-Menten analysis of the transport rates with varying R6G concentrations for wild type Pdr5 and the different mutants.  $V_{max}$  values were calculated by measuring the relative percent of R6G transported at the end of 700 s.

Mutant	$K_m$	$V_{max}$
	<i>nM</i>	relative transport of R6G %
Pdr5 WT	20.1 $\pm$ 2.9	83.52 $\pm$ 5.7
Walker A	25.3 $\pm$ 6.6	23.62 $\pm$ 2.7
Walker B	21.4 $\pm$ 3.3	61.44 $\pm$ 5.8
H-loop	18.7 $\pm$ 3.4	71.52 $\pm$ 9.7
C-loop	20.2 $\pm$ 7.5	36.40 $\pm$ 5.6
HC-loop	No transport	3.74 $\pm$ 0.80
AHC	No transport	2.33 $\pm$ 0.67
ABHC	No transport	0.68 $\pm$ 0.13

ATP in our case. The decrease in fluorescence intensity is a result of the formation of nonfluorescent excimers of R6G once transported inside the vesicle. As summarized in Fig. 5, all mutants except the HC-loop and AHC and ABHC mutants were able to efficiently transport R6G, although at different rates inside the vesicle. The affinities of these mutants toward R6G are summarized in Table 4. As seen, the  $K_m$  values are identical within experimental error for all mutants except for those that are impaired in R6G transport, but  $V_{max}$  values display considerable variation representing differential effects of the point mutations on the rate of substrate transport.

**Visualization of R6G Accumulation in Whole Cells**—When compared with the liquid drug resistance results of R6G, one has to stress that some mutants displayed better resistance than wild type Pdr5 but did not transport R6G in the *in vitro* transport assay. To investigate this disparity, we visualized R6G accumulations in yeast cells in the presence of R6G using fluorescence microscopy. As demonstrated in Fig. 6, *a* and *b*, cells lacking Pdr5 ( $\Delta pdr5$ ) clearly displayed an accumulation of the dye within the cells, whereas wild type cells efficiently transported R6G out of the cells as no R6G fluorescence could be detected within the cells (Fig. 6, *c* and *d*). Cells expressing the C199K mutation of Pdr5 (Walker A mutant), which are comparatively less efficient than the wild type cells in transporting

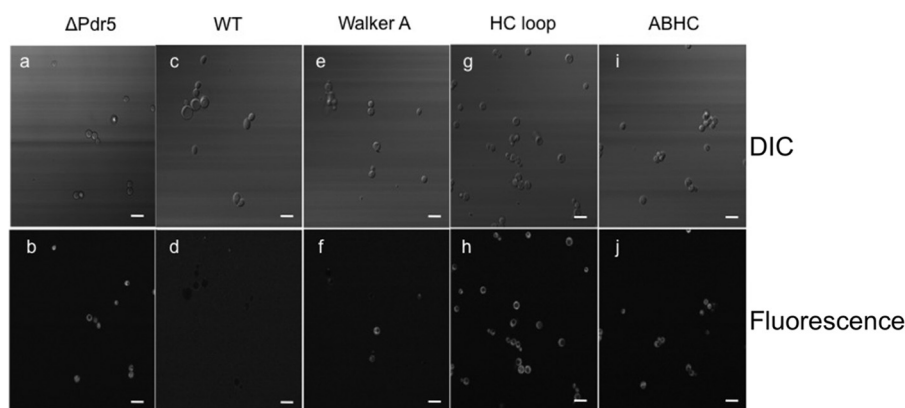


FIGURE 6. *In vivo* accumulation of R6G within selective Pdr5 mutants. *S. cerevisiae* cells from the liquid drug assay microtiter plates after 48 h of incubation at 30 °C were observed for R6G accumulation using a Zeiss LSM 780 microscope. Upper panels (a, c, e, g, and i) display differential interference contrast (DIC) images, and the lower panels (b, d, f, h, and j) display the corresponding fluorescent images. Bright fluorescence indicates rhodamine accumulation within cells. The final R6G concentration in the cells was 10.6  $\mu\text{g/ml}$ . Bar represents length of 10  $\mu\text{m}$ .

R6G (Fig. 5), displayed accumulation of the dye but to a reduced extent as compared with the knock-out strain (Fig. 6, e and f). In contrast, the HC-loop and the ABHC mutants, which displayed higher resistance toward R6G in the liquid drug assays (Fig. 2), demonstrated accumulation of the drug within the cells while maintaining cell viability (Fig. 6, g–j). This strongly suggests that compensatory mechanisms apart from transport of the substrate outside the cell play a significant role in the resistance toward the drug in these specific mutants and explains the disparity between the transport and liquid drug assays.

## DISCUSSION

Asymmetry in NBS is a feature not exclusively observed in fungal ABC transporters. Rather a number of human ABC transporters display this degeneration as well. Our observations with Pdr5 after exchange of degenerate residues with consensus ones provide strong evidence that the degenerated site is indeed optimized to structurally and functionally support ATP hydrolysis occurring at the opposite end. It has been proposed for a number of asymmetric transporters, such as the cystic fibrosis transmembrane regulator along with fungal ABC transporters, that the degenerated site might act as a platform for ATP hydrolysis at the consensus site (10, 28). This theory gains more support from our observations that, in an attempt to make the degenerate site capable of ATP hydrolysis, renders the protein completely nonfunctional in terms of ATP hydrolysis as well as substrate transport.

These observations also point in the direction of subtle inter- and intradomain communication necessary for the protein to fuel substrate transport with the energy of ATP hydrolysis. For an ABC transporter to function properly, a number of structural elements have been proposed to play key roles in the “chain of communication” necessary for optimal activity. Among these, the D-loops are involved in *trans*-interactions within the NBDs, especially as the Asp residue from the consensus sequence has been shown to interact with the Ser residue of the Walker A in the opposite NBD (25). D-loops are also proposed to be the sensors and communicators between the NBSs where they can communicate ATP binding and hydrolysis at one site to the other site (29). The Q-loop Gln residue has been proposed to be important in coordinating the water mol-

ecule in the active site during ATP hydrolysis (22). The Q-loops have also been proposed to be essential for conformational coupling of movements in NBDs to the TMDs in P-gp (30); interestingly, in Mrp1 it was observed that the Q-loops did not play an essential role in interdomain communication (31). As seen from the homology model of Pdr5 (32) based on the crystal structures of Sav1866 (33) and mouse P-gp (34), it is plausible that the Q-loops in Pdr5 might play a role in interdomain communication (26). In addition to these are the coupling helices that are one of the most structurally distinct elements in this communication pathway. They are like the gatekeepers guarding the substrate binding pocket as well as the anchors of the TMDs fitting in the sockets of NBDs (35). The X-loop Glu residues are also potentially important in the communication pathway because of their placement right near the substrate binding pocket as was first observed in the Sav1866 structure (33), but not enough studies have been carried out on its precise role so far.

We believe that in our “regenerated” Pdr5, it is this very communication within the NBDs and, in turn, from the NBDs to the TMDs that is disrupted by vast changes in the degenerate NBS. This hypothesis is also supported by the recent study carried out on the D-loops of Pdr5 by Furman *et al.* (36) where its role in intradomain signaling was studied. As seen from the observations, individual mutations, *viz.* Walker A, Walker B, H-loop, and C-loop, are tolerated. ATP hydrolysis is not greatly affected in these mutants, and R6G transport is also evident, although with varying degrees compared with the wild type. However, as these mutations are combined, *viz.* HC-loop, AHC-loop, and ABHC-loop, it first leads to lack of R6G transport (HC-loop) (Table 4) and later to a drastic decrease in ATP hydrolysis (AHC- and ABHC-loops) (Tables 3 and 4). The HC-loop mutant is particularly interesting because it displays a lack of substrate transport for R6G despite the close wild type levels of ATPase activity. This indicates that the two events of ATP hydrolysis and substrate transport are indeed uncoupled at least for R6G in this mutant. In our opinion, the major effect of changes in the degenerate site due to amino acid alterations is the breakdown of communication between the two NBSs and the NBS(s) and TMD(s). This is more severe in the case of the

## Role of Degenerate Nucleotide-binding Site in Pdr5

AHC-loop and the ABHC-loop mutants, and hence, it hampers ATP hydrolysis even at the consensus NBS that was untouched in this study.

In our view, Pdr5 like other yeast ABC transporters has evolved a structural architecture consisting of a degenerate NBS, and the entire intra- and interdomain communications involving D-, Q-, and X-loops are in place and optimized taking into account one consensus and one degenerate NBS. Our study of mutating the residues involved in the degenerate site altered the communication between the two NBS and hence affected the ATP hydrolysis occurring at the consensus NBS. Taking into consideration biochemical evidence from asymmetric transporters does imply the necessity of a “quiet” platform at the degenerate NBS where nucleotide exchange might occur but much less frequently as compared with the consensus NBS. When we make this quiet site more flexible by careful exchange of key residues, it seems to be tolerated to an extent, in case of Pdr5 up to the C-loop, but further changes disrupt ATP hydrolysis completely.

In the liquid resistance assays (Fig. 2), it was observed that the completely regenerated Pdr5 was clearly at a disadvantage in providing resistance to the yeast cells when challenged with different drugs. The big exception was R6G where resistance was slightly better as compared with WT. This observation, although primary, tells us that restoring all residues back to the consensus sequence does more harm to the protein than being beneficial. When compared with the liquid resistance assay results for R6G, the AHC mutant is indeed worse than WT in imparting resistance. But the HC-loop and ABHC-loop mutants do display increased resistance toward R6G in the liquid resistance assay. This is contradictory to our observation in the R6G transport assays where these two mutants do not display any transport of rhodamine in membrane vesicles. To investigate this contradiction, we employed microscopic techniques to directly observe R6G in whole cells. Pdr5WT (Fig. 6, *c* and *d*) and  $\Delta$ Pdr5 (Fig. 6, *a* and *b*) were our positive and negative controls, respectively. As can be clearly observed, the WT cells that can actively transport R6G outside show no accumulation of the dye within the cells, although the knock-out strain accumulates the dye in the absence of the transporter. The Walker A mutant, C199K (Fig. 6, *e* and *f*), which is deficient in R6G transport, displays few cells, which accumulate the dye, whereas the HC (Fig. 6, *g* and *h*) and ABHC (Fig. 6, *i* and *j*) mutants show a large number of cells, which have accumulation of the dye inside the cells. Differential interference contrast images of these cells also confirmed that these cells were alive. These observations point toward compensatory mechanisms, which come into play only when a transport inefficient protein is present in the cell, as the knock-out and the WT strains do not display such behavior. We can therefore rule out the possibility of additional transporters being up-regulated in the HC and ABHC mutants to pump out the substrate that might lead to increased resistance toward R6G as seen in the liquid drug tests. However, further investigations, which are beyond the scope of this study, are required to explain this observation at a protein level.

Here, we have presented the first comprehensive study of systematically replacing each degenerate amino acid residue

involved in ATP binding and hydrolysis in Pdr5 with its consensus counterpart. The completely regenerated Pdr5 protein was functionally severely impaired as seen with ATP hydrolysis and *in vitro* transport experiments. This leads us to conclude that maintaining a degenerate ATP hydrolysis site seems essential for the optimal functioning of Pdr5 from an energetic and also evolutionary point of view. It is also plausible that for ABC transporters harboring a degenerate NBS that is incapable of hydrolyzing ATP could lead to high basal ATPase activity occurring at the consensus site. This, in turn, is a possible explanation as to why some ABC transporters have and continue to maintain a degenerate site. The trade-off between constant ATP hydrolysis at only one site instead of two leads to the protein being ready at all times to protect the cell against xenotoxic compounds without delay. This, to our knowledge, is a significant deviation from ABC transporters having both NBS capable of ATP hydrolysis and displaying substrate stimulation and validates further investigation.

---

*Acknowledgments*—We thank Katerina Krikoni, Marianne Kluth, and Martha Swiatek for important support at various stages of the project. We are indebted to Robert Ernst (University of Frankfurt) and Karl Kuchler (Medical University of Vienna) for important contributions at an early stage of the project and for many fruitful and stimulating discussions. We also thank Peter Zentis and Stephanie Weidtkamp-Peters for invaluable support in the LSM measurements.

---

## REFERENCES

1. Erkens, G. B., Majsnerowska, M., ter Beek, J., and Slotboom, D. J. (2012) Energy coupling factor-type ABC transporters for vitamin uptake in prokaryotes. *Biochemistry* **51**, 4390–4396
2. Hinz, A., and Tampé, R. (2012) ABC transporters and immunity: mechanism of self-defense. *Biochemistry* **51**, 4981–4989
3. Klein, C., Kuchler, K., and Valachovic, M. (2011) ABC proteins in yeast and fungal pathogens. *Essays Biochem.* **50**, 101–119
4. Prasad, R., and Goffeau, A. (2012) Yeast ATP-binding cassette transporters conferring multidrug resistance. *Annu. Rev. Microbiol.* **66**, 39–63
5. Sharom, F. J. (2011) The P-glycoprotein multidrug transporter. *Essays Biochem.* **50**, 161–178
6. Golin, J., Ambudkar, S. V., and May, L. (2007) The yeast Pdr5p multidrug transporter: how does it recognize so many substrates? *Biochem. Biophys. Res. Commun.* **356**, 1–5
7. Ernst, R., Klemm, R., Schmitt, L., and Kuchler, K. (2005) Yeast ATP-binding cassette transporters: cellular cleaning pumps. *Methods Enzymol.* **400**, 460–484
8. Kolaczowski, M., van der Rest, M., Cybularz-Kolaczowska, A., Soumillion, J. P., Konings, W. N., and Goffeau, A. (1996) Anticancer drugs, ionophoric peptides, and steroids as substrates of the yeast multidrug transporter Pdr5p. *J. Biol. Chem.* **271**, 31543–31548
9. Goffeau, A., and Dufour, J. P. (1988) Plasma membrane ATPase from the yeast *Saccharomyces cerevisiae*. *Methods Enzymol.* **157**, 528–533
10. Ernst, R., Kueppers, P., Klein, C. M., Schwarzmueller, T., Kuchler, K., and Schmitt, L. (2008) A mutation of the H-loop selectively affects rhodamine transport by the yeast multidrug ABC transporter Pdr5. *Proc. Natl. Acad. Sci. U.S.A.* **105**, 5069–5074
11. Shapiro, A. B., and Ling, V. (1998) The mechanism of ATP-dependent multidrug transport by P-glycoprotein. *Acta Physiol. Scand. Suppl.* **643**, 227–234
12. Zaitseva, J., Jenewein, S., Oswald, C., Jumpertz, T., Holland, I. B., and Schmitt, L. (2005) A molecular understanding of the catalytic cycle of the nucleotide-binding domain of the ABC transporter HlyB. *Biochem. Soc. Trans.* **33**, 990–995
13. Hanekop, N., Zaitseva, J., Jenewein, S., Holland, I. B., and Schmitt, L.

- (2006) Molecular insights into the mechanism of ATP-hydrolysis by the NBD of the ABC-transporter HlyB. *FEBS Lett.* **580**, 1036–1041
14. Linton, K. J. (2007) Structure and function of ABC transporters. *Physiology* **22**, 122–130
  15. Lamping, E., Baret, P. V., Holmes, A. R., Monk, B. C., Goffeau, A., and Cannon, R. D. (2010) Fungal PDR transporters: Phylogeny, topology, motifs and function. *Fungal Genet. Biol.* **47**, 127–142
  16. Csanády, L., Mihályi, C., Szollosi, A., Töröcsik, B., and Vergani, P. (2013) Conformational changes in the catalytically inactive nucleotide-binding site of CFTR. *J. Gen. Physiol.* **142**, 61–73
  17. Decottignies, A., Kolaczowski, M., Balzi, E., and Goffeau, A. (1994) Solubilization and characterization of the overexpressed PDR5 multidrug resistance nucleotide triphosphatase of yeast. *J. Biol. Chem.* **269**, 12797–12803
  18. Wada, S., Niimi, M., Niimi, K., Holmes, A. R., Monk, B. C., Cannon, R. D., and Uehara, Y. (2002) *Candida glabrata* ATP-binding cassette transporters Cdr1p and Pdh1p expressed in a *Saccharomyces cerevisiae* strain deficient in membrane transporters show phosphorylation-dependent pumping properties. *J. Biol. Chem.* **277**, 46809–46821
  19. Dufour, J. P., Amory, A., and Goffeau, A. (1988) Plasma membrane ATPase from the yeast *Schizosaccharomyces pombe*. *Methods Enzymol.* **157**, 513–528
  20. Zaitseva, J., Holland, I. B., and Schmitt, L. (2004) The role of CAPS buffer in expanding the crystallization space of the nucleotide-binding domain of the ABC transporter haemolysin B from *Escherichia coli*. *Acta Crystallogr. D Biol. Crystallogr.* **60**, 1076–1084
  21. Vetter, I. R., and Wittinghofer, A. (1999) Nucleoside triphosphate-binding proteins: different scaffolds to achieve phosphoryl transfer. *Q. Rev. Biophys.* **32**, 1–56
  22. Smith, P. C., Karpowich, N., Millen, L., Moody, J. E., Rosen, J., Thomas, P. J., and Hunt, J. F. (2002) ATP binding to the motor domain from an ABC transporter drives formation of a nucleotide sandwich dimer. *Mol. Cell* **10**, 139–149
  23. Chen, J., Sharma, S., Quioco, F. A., and Davidson, A. L. (2001) Trapping the transition state of an ATP-binding cassette transporter: evidence for a concerted mechanism of maltose transport. *Proc. Natl. Acad. Sci. U.S.A.* **98**, 1525–1530
  24. Oldham, M. L., and Chen, J. (2011) Snapshots of the maltose transporter during ATP hydrolysis. *Proc. Natl. Acad. Sci. U.S.A.* **108**, 15152–15156
  25. Zaitseva, J., Jenewein, S., Jumpertz, T., Holland, I. B., and Schmitt, L. (2005) H662 is the linchpin of ATP hydrolysis in the nucleotide-binding domain of the ABC transporter HlyB. *EMBO J.* **24**, 1901–1910
  26. Ananthaswamy, N., Rutledge, R., Sauna, Z. E., Ambudkar, S. V., Dine, E., Nelson, E., Xia, D., and Golin, J. (2010) The signaling interface of the yeast multidrug transporter Pdr5 adopts a cis conformation, and there are functional overlap and equivalence of the deviant and canonical Q-loop residues. *Biochemistry* **49**, 4440–4449
  27. Serrano, R. (1988) H<sup>+</sup>-ATPase from plasma membranes of *Saccharomyces cerevisiae* and *Avena sativa* roots: purification and reconstitution. *Methods Enzymol.* **157**, 533–544
  28. Basso, C., Vergani, P., Nairn, A. C., and Gadsby, D. C. (2003) Prolonged nonhydrolytic interaction of nucleotide with CFTR's NH<sub>2</sub>-terminal nucleotide binding domain and its role in channel gating. *J. Gen. Physiol.* **122**, 333–348
  29. Jones, P. M., and George, A. M. (2012) Role of the D-loops in allosteric control of ATP hydrolysis in an ABC transporter. *J. Phys. Chem. A* **116**, 3004–3013
  30. Urbatsch, I. L., Gimi, K., Wilke-Mounts, S., and Senior, A. E. (2000) Investigation of the role of glutamine-471 and glutamine-1114 in the two catalytic sites of P-glycoprotein. *Biochemistry* **39**, 11921–11927
  31. Yang, R., Hou, Y. X., Campbell, C. A., Palaniyandi, K., Zhao, Q., Bordner, A. J., and Chang, X. B. (2011) Glutamine residues in Q-loops of multidrug resistance protein MRP1 contribute to ATP binding via interaction with metal cofactor. *Biochim. Biophys. Acta* **1808**, 1790–1796
  32. Rutledge, R. M., Esser, L., Ma, J., and Xia, D. (2011) Toward understanding the mechanism of action of the yeast multidrug resistance transporter Pdr5p: a molecular modeling study. *J. Struct. Biol.* **173**, 333–344
  33. Dawson, R. J., and Locher, K. P. (2006) Structure of a bacterial multidrug ABC transporter. *Nature* **443**, 180–185
  34. Aller, S. G., Yu, J., Ward, A., Weng, Y., Chittaboina, S., Zhuo, R., Harrel, P. M., Trinh, Y. T., Zhang, Q., Urbatsch, I. L., and Chang, G. (2009) Structure of P-glycoprotein reveals a molecular basis for poly-specific drug binding. *Science* **323**, 1718–1722
  35. Locher, K. P. (2009) Review. Structure and mechanism of ATP-binding cassette transporters. *Philos. Trans. R. Soc. Lond. B Biol. Sci.* **364**, 239–245
  36. Furman, C., Mehla, J., Ananthaswamy, N., Arya, N., Kulesh, B., Kovach, I., Ambudkar, S. V., and Golin, J. (2013) The deviant ATP-binding site of the multidrug efflux pump Pdr5 plays an active role in the transport cycle. *J. Biol. Chem.* **288**, 30420–30431